Competition of Percolation and Phase Separation in a Fluid of Adhesive Hard Spheres

Mark A. Miller and Daan Frenkel

FOM Institute for Atomic and Molecular Physics, Kruislaan 407, 1098 SJ Amsterdam, The Netherlands
(Received 6 December 2002; published 4 April 2003)

Using a combination of Monte Carlo techniques, we locate the liquid-vapor critical point of adhesive hard spheres. We find that the critical point lies deep inside the gel region of the phase diagram. The (reduced) critical temperature and density are $\tau_c = 0.1133 \pm 0.0005$ and $\rho_c = 0.508 \pm 0.01$. We compare these results with the available theoretical predictions. Using a finite-size scaling analysis, we verify that the critical behavior of the adhesive hard sphere model is consistent with that of the 3D Ising universality class, the default for systems with short-range attractive forces.

The structure of a simple liquid is well described by that of a system of hard spheres at the same effective density. To a good approximation, the effect of attractive interactions on the liquid structure can be ignored. This feature of simple liquids is implicit in the van der Waals theory for the liquid-vapor transition, and has been made explicit in the highly successful thermodynamic perturbation theories for simple liquids [1]. The perturbation approach becomes exact as the range of the attractive interaction tends to infinity while its integrated strength remains constant [2]. We refer to this limit as the "van der Waals" (VDW) limit [3]. Conversely, as the attractive forces become shorter ranged and stronger, the perturbation approach is likely to break down. Fluids with strong, short-ranged attraction (so-called "energetic" fluids [4]) are of growing importance in the area of complex liquids. For example, short-range attractions are thought to be responsible for the transition from a "repulsive" to an "attractive" glass [5], which has recently been observed experimentally in PMMA (polymethylmethacrylate) dispersions [6].

In this Letter, we consider a model system that can be considered as the prototypical energetic fluid: a fluid of adhesive hard spheres (AHS). Introduced in 1968 [7], the AHS model is a reference system for particles with short-range attractions. The pair potential consists of an impenetrable core plus a surface adhesion term that favors configurations where spheres are in contact. At larger separations, there is no interaction. The AHS model can be considered as the "anti–van der Waals" limit. Baxter solved the Percus-Yevick (PY) equation for the AHS model analytically [7]. In fact, his solution is often used to analyze experimental results for systems as diverse as silica suspensions [8], copolymer micelles [9], and the fluid phase of lysozyme [10].

One important feature of the AHS model is that its phase diagram contains a liquid-vapor coexistence region [11]. The PY equation offers different routes to estimate the location of the liquid-vapor critical point. However, the "compressibility route" [7] and the "energy route" [12] lead to estimates for the critical temperature that

differ by some 20%, while the estimates for the critical density differ by almost a factor of 3. For the analysis of experimental data, it is important to know the location of the critical point more accurately since, upon cooling, adhesive hard spheres percolate to form a gel. The location of the percolation curve is available from simulation [13,14] and from analytical estimates [15]. It is not clear, though, how percolation interferes with the fluid-fluid phase separation. If Baxter's estimate of the critical point were right, the critical point would be on, or near, the percolation curve. However, if the estimate of Ref. [12] were closer to reality, then the fluid-fluid critical point would be deep inside the gel phase. Clearly, this difference has implications for the possibility of observing the fluid-fluid critical point in systems with short-ranged attraction. Also for the (attractive) glass transition, it makes a considerable difference whether or not the transition line runs close to a liquid-vapor critical point.

In spite of its obvious importance as a reference system for energetic (as contrasted to "entropic") complex liquids [4], there exist, to our knowledge, no accurate numerical estimates of the critical point of the AHS model. This is not surprising, as computer simulations of the low-temperature AHS model are notoriously difficult, due to its propensity to form large, even percolating, clusters. In this Letter, we report a Monte Carlo (MC) simulation study that allows us to locate the AHS critical point.

The AHS interaction can be derived from a square well potential by taking a limit in which the well becomes infinitesimally narrow and simultaneously infinitely deep such that the integrated Boltzmann weight of bound configurations remains finite [7]. The interaction is most easily defined by the expression for the Boltzmann factor as a function of pair separation, r:

$$\exp[-U(r)/kT] = \Theta(r - \sigma) + \frac{\sigma}{12\tau}\delta(r - \sigma). \quad (1)$$

In Eq. (1), $U(r)$ and kT are the formal pair potential and thermal energy, respectively, while σ is the hard core diameter, which we henceforth use as the unit of length.

The step function Θ accounts for the hard sphere repulsion, and the Dirac delta function introduces the surface adhesion. The parameter τ determines the strength of the adhesion and can be interpreted as an effective temperature, or an "inverse stickiness parameter."

To compare the properties of the AHS and VDW models, we need a measure for the strength of the attractive interactions that is meaningful in both limits. This is best achieved by comparing the reduced second virial coefficients: $B_2^* \equiv B_2/B_2^{HS}$, where B_2^{HS} is the second virial coefficient of hard spheres. For the AHS model, $B_2^* = 1 - 1/(4\tau)$, and we use this expression to define the τ parameter for the VDW model. In the VDW limit, the free-energy density is given by $f_{VDW}(\rho) = f_{HS}(\rho) - a\rho^2$, where f_{HS} is the free-energy density of a system of hard spheres at density ρ, while the constant a measures the strength of the attractive forces. Hence, in the VDW limit, $\tau = kTB_2^{HS}/(4a)$ is proportional to the temperature. We henceforth refer to τ as the temperature parameter for both the VDW and AHS systems.

In the AHS model, particles may stick and form clusters. At sufficiently low τ, clusters may percolate (span the system), mimicking the infinite clusters that form during gelation in the real system. Percolating clusters pose serious problems for any simulation scheme that employs volume changing moves (e.g., constant pressure MC), since all such moves are rejected as soon as percolating clusters appear. To study the phase behavior of adhesive hard spheres, we therefore used grand canonical MC (GCMC) simulation, which can be used beyond the percolation threshold. Yet, even with GCMC, equilibration of the system at low temperatures is prohibitively slow. We therefore combine GCMC with parallel tempering to speed up equilibration, and with multiple histogram reweighting, to make optimal use of the available simulation data. All simulation techniques had to be specifically adapted for the AHS model.

The fact that the attractive term in Eq. (1) is infinitesimally narrow means that, in a simulation, the chance of generating a bound configuration by random displacement of a particle is vanishingly small. Conversely, the probability of breaking such a bond, once formed, is also negligible. Consequently, conventional Metropolis sampling cannot be applied to the AHS model.

We therefore employ a modification of the AHS-MC schemes described in Ref. [13], where single particle displacements explicitly make and break up to three contacts with the test particle simultaneously. States with higher coordination numbers can be reached indirectly through suitable combinations of moves.

In our GCMC simulations, we employ particle insertion and removal steps with equal probability that together constitute 45% of MC steps. We only insert and remove particles that are not bound to others. To speed up equilibration, we perform cluster translation moves with probability 5%. A particle is chosen at random, and the

cluster to which it belongs is translated by a random amount in each Cartesian direction up to a maximum that is inversely proportional to the number of particles in the cluster.

To overcome the slow equilibration of large clusters at low τ or high density, we have used the parallel tempering scheme of Geyer [16]. Parallel tempering can be performed with replicas at different temperatures, different chemical potentials, or combinations of both. We have found it most convenient to gather statistics across the full density range for one temperature at a time, and therefore chose to run a hierarchy of chemical potentials, μ, with the same value of τ. Each replica attempts a configuration exchange with one of its neighbors in μ (alternating between the higher and lower neighbor) every 200 MC steps. The acceptance probability for an exchange between replicas i and j is $\min[1, (z_i/z_j)^{N_j-N_i}]$, where N_i is the number of particles in the current configuration of replica i, and the activity z is related to the chemical potential by $z = \Lambda^{-3}\exp(\mu/kT)$, with Λ the thermal de Broglie wavelength.

The final computational tool needed to analyze the data is multiple histogram reweighting [17]. The probability of observing the system in a state with N particles and B binary contacts between the particles at temperature τ and activity z can be exactly decomposed into the form

$$p_{NB}(\tau, z) = \Omega_{NB}\tau^{-B}z^N/\Xi(\tau, z), \qquad (2)$$

where Ω_{NB} is an effective density of states, and $\Xi(\tau, z)$ is the grand canonical partition function. Knowledge of Ω_{NB} up to a multiplicative constant is sufficient to calculate the distribution of N or B at any set of conditions (τ, z). Ω_{NB} can be obtained over a wide range of (N, B) by combining overlapping two-dimensional histograms of N and B collected from simulations at different τ and z.

Simulations at sufficiently low τ show a range of activities in which the density distribution is bimodal, indicating the coexistence of a high- and a low-density fluid phase. We studied this coexistence at four different system sizes, labeled by the length L of the cubic simulation box. For $L = 5, 6,$ and 8, the simulations consisted of 10^6 equilibration blocks and 10^7 acquisition blocks, where a block is L^3/σ^3 MC trial moves, each of which may be a particle displacement, particle insertion/removal, cluster translation, or replica exchange. At each temperature, seven or eight parallel replicas were used, with the range of activities chosen to span the coexisting densities. At $L = 10$, the numbers of equilibration and acquisition blocks had to be lowered to 2.5×10^5 and 2.5×10^6, respectively, to obtain results in a reasonable computational time.

The (N, B) histograms for different τ and z were combined for each system size separately. The coexisting densities were then obtained as a function of temperature by reweighting the histograms to find the activity at

which the two density peaks have equal height. Given the near-symmetrical density distribution, this criterion is met when the peak volumes are also almost equal. However, the equal height method is less ambiguous when the peaks overlap, as here. Figure 1 shows the coexistence curves, which clearly exhibit strong finite-size effects. The curves obtained at different L coincide at sufficiently low temperature, but deviate significantly from each other as the critical region is approached.

The size dependence of the coexistence distributions can be used to locate the critical point more accurately using the approach developed by Bruce and Wilding [18,19]. This method uses the fact that, within a universality class, the critical distribution of the order parameter is invariant up to a rescaling of the order parameter. As the AHS interactions are short ranged, the fluid-fluid critical point of this model is expected to belong to the 3D Ising universality class. The critical distribution is known to high precision from studies of lattice systems, and accurate analytic fits are available [20].

The slight asymmetry of the density distribution reflects the absence of particle-hole symmetry in off-lattice models. A symmetrical distribution can be recovered by accounting for the mixed character of the scaling fields. The appropriate order parameter is then no longer the pure particle density $\rho = N/L^3$, but includes a contribution from the energy density, which in the AHS model can be taken as $u = -B/L^3$. The particle and energy density operators are replaced by the linear combinations [18]

$$\mathcal{E} = \frac{u - r\rho}{1 - sr} \qquad \mathcal{M} = \frac{\rho - su}{1 - sr}, \qquad (3)$$

where s and r are system-dependent field mixing parameters that are identically zero for models with Ising symmetry. Precisely at criticality, the distribution of $\mathcal{M}$ in a sys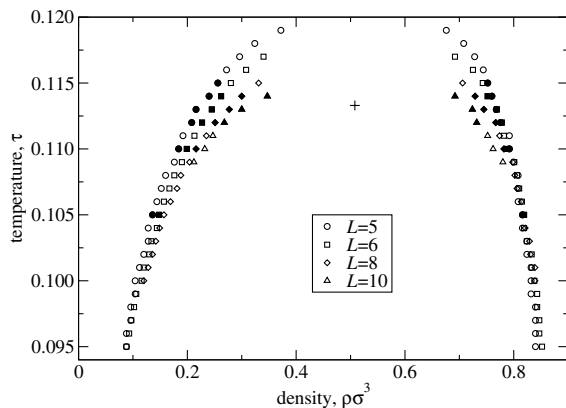tem of sufficiently large linear length L takes on the universal form $p_L(\mathcal{M}) = p^*(a_L[\mathcal{M} - \mathcal{M}_c])$, where $\mathcal{M}_c = \langle \mathcal{M} \rangle$ evaluated at the critical temperature, and $a_L \propto L^{\beta/\nu}$ with β and ν critical exponents.

Table I lists the apparent critical temperature τ_a and mixing parameter s at which the distribution of $\mathcal{M}$ most closely matches $p^*(x)$ for the four system sizes studied. The fact that s is small indicates that the distribution of ρ itself is nearly symmetric. The apparent size dependence of s is probably—at least partly—due to the fact that, despite the long simulations employed, statistical fluctuations in the histograms are still significant. For small L, τ_a is expected to show some size dependence due to finite-size corrections to scaling [19]. However, the differences in τ_a shown in Table I are not monotonic, and are again likely to be due to limited statistics. Rather than attempting to extrapolate to the infinite system limit, we therefore quote the critical parameters that most closely reproduce the universal critical form, with error bars covering the uncertainty in a typical $\tau_a(L)$, plus the range of values observed for different L:

$$\tau_c^{\text{sim}} = 0.1133 \pm 0.0005, \qquad \rho_c^{\text{sim}} = 0.508 \pm 0.01.$$

Figure 2 shows the distribution of the order parameter at the proposed τ_c^{sim} (not the individual apparent critical temperatures τ_a) for all four system sizes. The collapse of the data onto the Ising distribution shows that the transition is consistent with this universality class.

The size dependence of the scaling factor a_L in Table I permits an estimate of the ratio of the critical exponents β and ν. A straightforward fit to the asymptotic form $a_L \propto L^{\beta/\nu}$ yields $\beta/\nu = 0.50 \pm 0.04$, which is clearly compatible with the Ising value $\beta/\nu = 0.52$.

We can now compare our numerical results with various theoretical predictions. Below, we list the estimates based on the PY compressibility [7] and energy [12] routes, and the estimate based on the VDW (mean-field) expression [21]:

$$\tau_c^{\text{PYc}} = 0.0976, \qquad \tau_c^{\text{PYe}} = 0.1185, \qquad \tau_c^{\text{VDW}} = 0.0943,$$
$$\rho_c^{\text{PYc}} = 0.232, \qquad \rho_c^{\text{PYe}} = 0.609, \qquad \rho_c^{\text{VDW}} = 0.250.$$

The coexistence curves for the two PY routes can be

FIG. 1. Coexistence curve of the AHS model from GCMC using four box lengths, L. Solid symbols denote points actually simulated; open symbols were obtained by histogram reweighting. Error bars are omitted for clarity. The cross denotes the estimated critical point at $\tau = 0.1133$, $\rho = 0.508$.

TABLE I. Size-dependent properties for critical point determination. τ_a is the apparent critical temperature, at which the distribution of $\mathcal{M}$ (with field-mixing parameter s) collapses onto the universal form $p^*(x)$. The remaining three columns refer to properties at the proposed critical temperature of $\tau_c^{\text{sim}} = 0.1133$: ρ_c is the mean density, z_c is the activity, and a_L scales $p(a_L \mathcal{M})$ to have unit variance.

L	s	τ_a	ρ_c	z_c	a_L
5	0.04	0.1130	0.499	0.088 09	3.830
6	0.04	0.1134	0.506	0.087 62	4.036
8	0.02	0.1135	0.513	0.087 27	4.727
10	0.02	0.1132	0.512	0.087 23	5.362

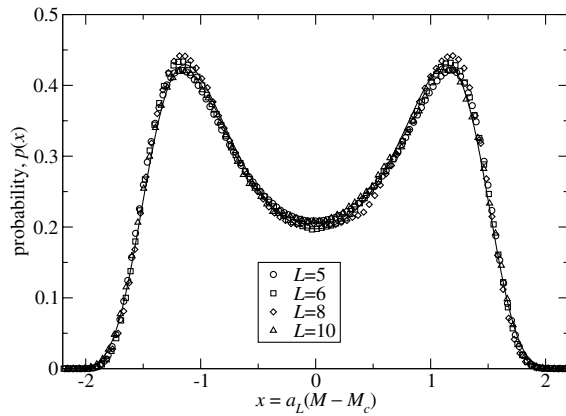FIG. 2. Distribution of the order parameter at the proposed critical temperature from GCMC at four different box lengths, L. Each curve has been scaled to have unit variance. The solid curve is the 3D Ising critical distribution [20].

obtained numerically using the analytical expressions [22] for the chemical potential and pressure. These theoretical curves, together with the mean-field result and the simulation data at $L = 8$ are shown in Fig. 3. The simulation results lie between the two PY predictions, but are clearly closer to those of the energy equation.

Also plotted in Fig. 3 is the percolation threshold. The theoretical result [15] corresponds to the PY estimate of where the cluster size diverges. In simulations, we define the percolation threshold as the locus of points were the probability of observing a percolating cluster in a canonical simulation is 50%. This definition is relatively size independent, and our results with $N = 500$ particles are consistent with the more elaborate analysis of Lee [14]. Both the theoretical and simulated percolation lines clearly show that the critical point of the fluid-fluid transition lies well within the percolated part of the phase diagram.
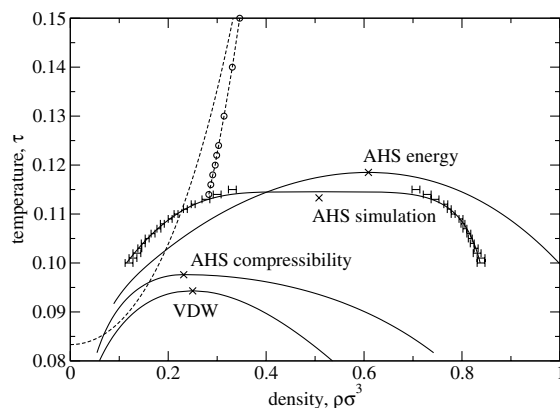

FIG. 3. Solid lines: coexistence curves for the VDW limit, the AHS PY compressibility, and energy routes, and AHS simulation with $L = 8$. For the latter, the line merely guides the eye between the data points. Dashed lines: percolation threshold from PY theory and simulation (line with circles).

The phase diagram reported in Fig. 3 is likely to be representative of that of real colloidal systems with short-ranged attraction at the same value of τ. If so, our findings suggest that the attractive glass transition [5,6] is relatively far removed from the fluid-fluid critical point.

[1] R. W. Zwanzig, J. Chem. Phys. **22**, 1420 (1954); J. A. Barker and D. Henderson, J. Chem. Phys. **47**, 4714 (1967); J. D. Weeks, D. Chandler, and H. C. Andersen, J. Chem. Phys. **54**, 5237 (1971).
[2] M. Kac, G. E. Uhlenbeck, and P. C. Hemmer, J. Math. Phys. (N.Y.) **4**, 216 (1963).
[3] In our definition of the VDW limit, we assume that the free-energy density of hard spheres is known exactly. Van der Waals used an approximate expression for this term.
[4] A. A. Louis, Philos. Trans. R. Soc. London A **359**, 939 (2001).
[5] K. Dawson *et al.*, Phys. Rev. E **63**, 011401 (2001).
[6] K. N. Pham *et al.*, Science **296**, 104 (2002).
[7] R. J. Baxter, J. Chem. Phys. **49**, 2770 (1968).
[8] S. Ramakrishnan *et al.*, J. Chem. Phys. **116**, 2201 (2002).
[9] F. Mallamace *et al.*, Physica (Amsterdam) **302A**, 202 (2001).
[10] R. Piazza, V. Peyre, and V. Degiorgio, Phys. Rev. E **58**, R2733 (1998).
[11] Stell [G. Stell, J. Stat. Phys. **63**, 1203 (1991)] has noted that the monodisperse AHS system is pathological: Very short-ranged attractions uniquely favor compact structures, such as the close-packed crystal. Freezing should preempt the liquid-vapor transition of monodisperse adhesive spheres. By making the spheres slightly polydisperse and taking the limit of vanishing well width, we can eliminate this problem.
[12] R. O. Watts, D. Henderson, and R. J. Baxter, Adv. Chem. Phys. **21**, 421 (1971).
[13] N. A. Seaton and E. D. Glandt, J. Chem. Phys. **86**, 4668 (1987); **87**, 1785 (1987); W. G. T. Kranendonk and D. Frenkel, Mol. Phys. **64**, 403 (1988).
[14] S. B. Lee, J. Chem. Phys. **114**, 2304 (2001).
[15] Y. C. Chiew and E. D. Glandt, J. Phys. A **16**, 2599 (1983).
[16] C. J. Geyer and E. A. Thompson, J. Am. Stat. Assoc. **90**, 909 (1995).
[17] A. M. Ferrenberg and R. H. Swendsen, Phys. Rev. Lett. **61**, 2635 (1988); **63**, 1195 (1989); S. Weerasinghe and F. G. Amar, J. Chem. Phys. **98**, 4967 (1993).
[18] A. D. Bruce and N. B. Wilding, Phys. Rev. Lett. **68**, 193 (1992).
[19] N. B. Wilding, Phys. Rev. E **52**, 602 (1995).
[20] M. M. Tsypin and H. W. J. Blöte, Phys. Rev. E **62**, 73 (2000).
[21] D. Frenkel *et al.*, Mol. Simul. **16**, 127 (1996).
[22] B. Barboy and R. Tenne, Chem. Phys. **38**, 369 (1979).